CHAPTER 3

SURFACE NANOSTRUCTURING OF Ti–6Al–4V THROUGH ULTRASONIC SHOT PEENING

3.1 INTRODUCTION

This chapter describes the effect of ultrasonic shot peening on microstructure modification, surface roughness and microhardness. Solution treated samples of the titanium alloy Ti–6Al–4V were subjected to ultrasonic shot peening (USSP) for different durations, from 0.25 to 30 minute, with hard steel balls of 3 mm diameter. The modification of microstructure was examined through optical, scanning and transmission electron microscopy. The shot peened surfaces were examined also by XRD for phase transformation, if any, resulting from USSP.

3.2 MICROSTRUCTURE CHARACTERIZATION

The microstructure of the alloy Ti–6Al–4V in the solution treated condition was studied by optical and scanning electron microscopy. Optical and SEM micrographs showed similar features of dual phase microstructure consisting of globular primary α and transformed β (Fig. 3.1).

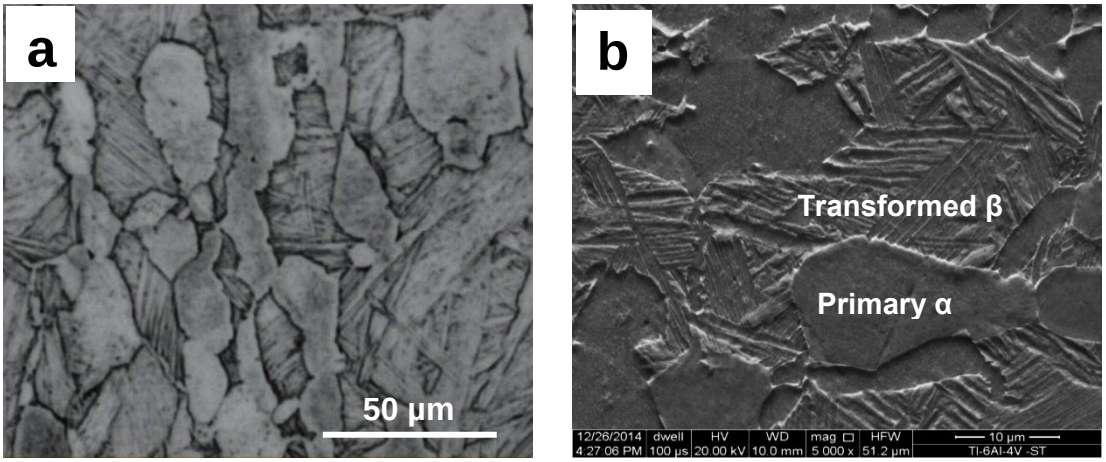

Fig. 3.1 Microstructure of solution treated alloy Ti–6Al–4V (a) optical (b) SEM.

3.2.1 *Optical Microscopy*

The typical optical micrographs of transverse section of the alloy Ti–6Al–4V, USSPed for 1, 5, 15 and 30 minute are shown in Fig. 3.2. The primary α and transformed β phases are uniformly distributed in the interior, below the dotted line, in the cross-section. The cross-sections of the USSPed samples show two distinct microstructures from the USSPed surface towards the interior; (1) deformed layer resulting from USSP and (2) the substrate.

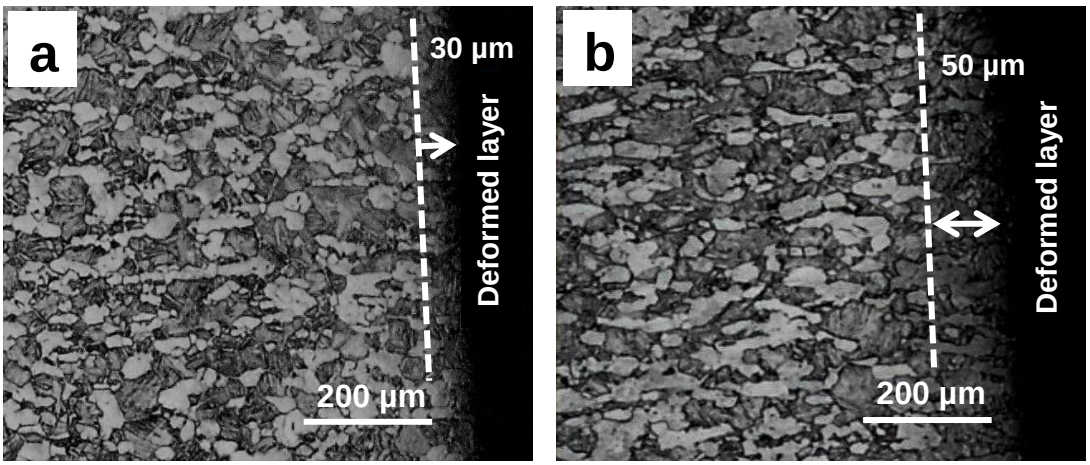

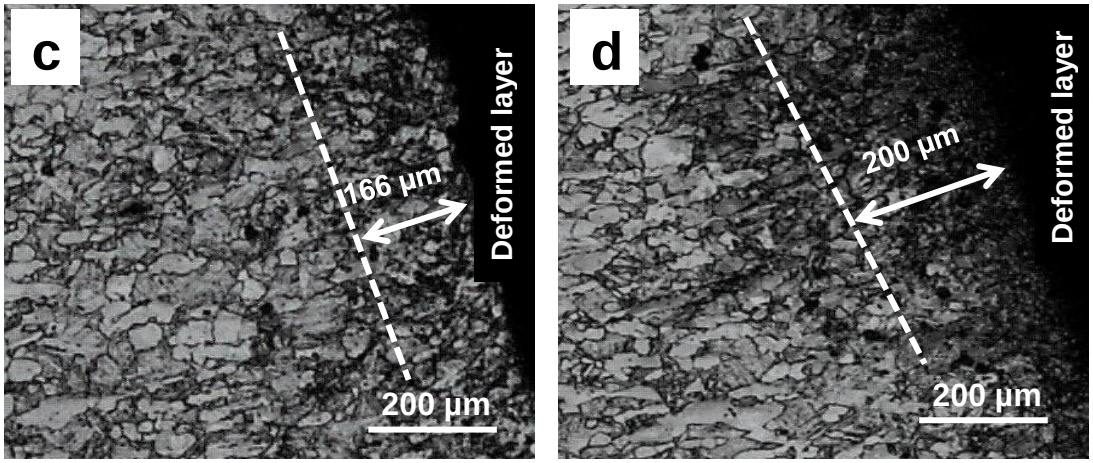

Fig. 3.2 Optical micrographs of cross-sections of the specimens USSPed for different durations: (a) 1 minute, (b) 5 minute, (c) 15 minute and (d) 30 minute.

Surface modification resulting from USSP is shown by these optical micrographs, up to the depths of ~30µm, ~50µm, ~166µm and ~200 µm from the shot peened surfaces of the samples USSPed, for 1, 5, 15 and 30 minute respectively.

3.2.2 Scanning Electron Microscopy

Surface morphology of the non-USSPed and USSPed samples was also examined by SEM. The typical surface morphologies of the non-USSPed and USSPed alloy Ti–6Al–4V are shown in Fig 3.3. SEM micrograph of the non-USSPed specimen shows the typical dual phase microstructure consisting of α and β phases, with globular morphology of primary α and transformed β (Fig 3.3a). It may be seen that dark contrast resulted from the USSP due to depression and cracking on the surface, in particular from the longer of USSP.

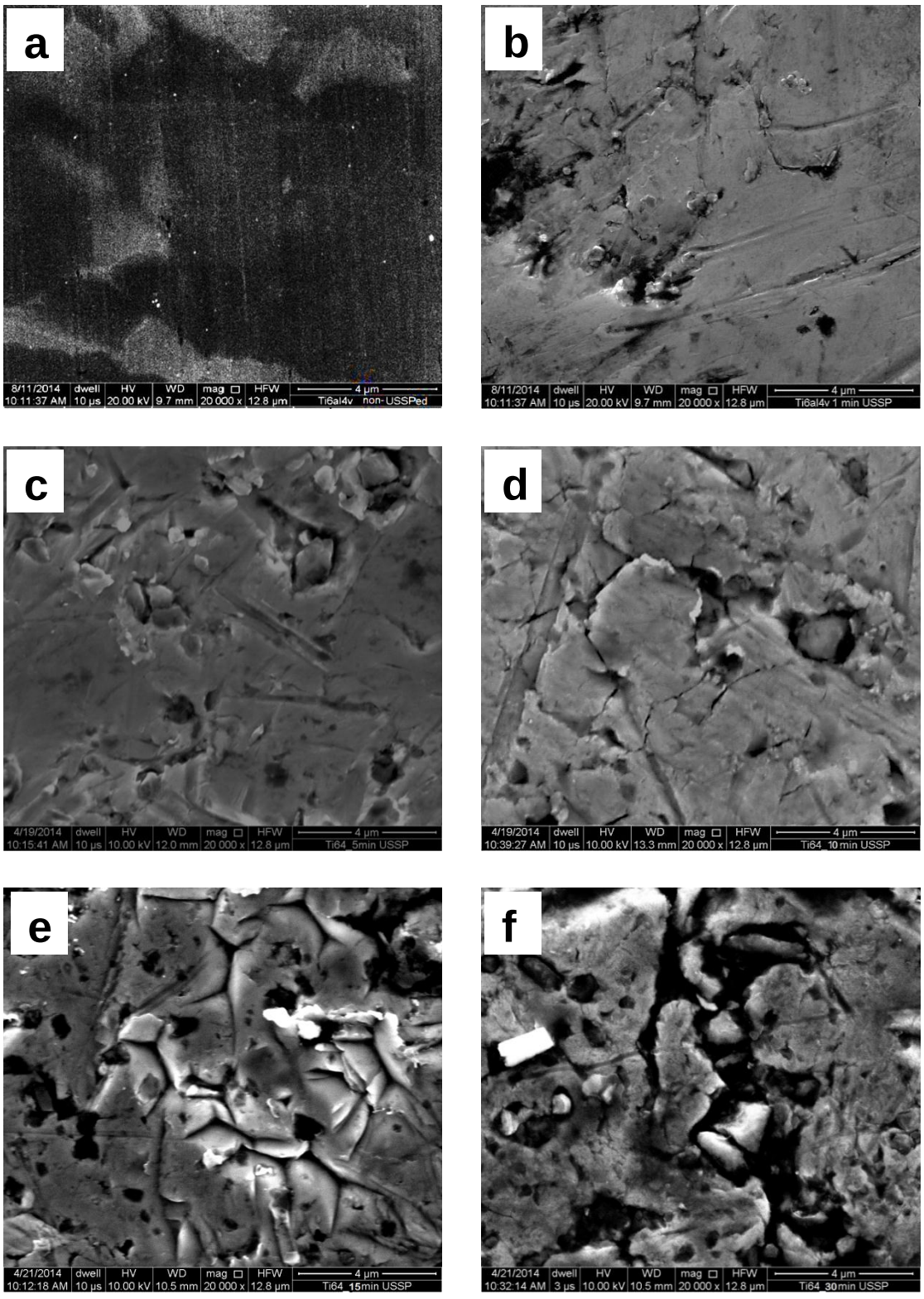

Fig. 3.3 SEM micrographs of the alloy Ti–6Al–4V: (a) non-USSPed, (b) 1 minute, (c) 5 minute, (d) 10 minute, (e) 15 minute and (f) 30 minute USSPed.

The cross-sections of the specimens USSPed for 5, 15, and 30 minute are shown in Figs. 3.4a, b and c respectively. Cracks may also be seen in some regions in Fig. 3.4c. The size of the constituent phases was reduced due to USSP in the surface region. There was no sign of any surface cracking in the specimens shot peened for short durations of 5 and 15 minute whereas there was surface cracking in the specimen USSPed for the longer duration of 30 minute (Fig. 3.4c).

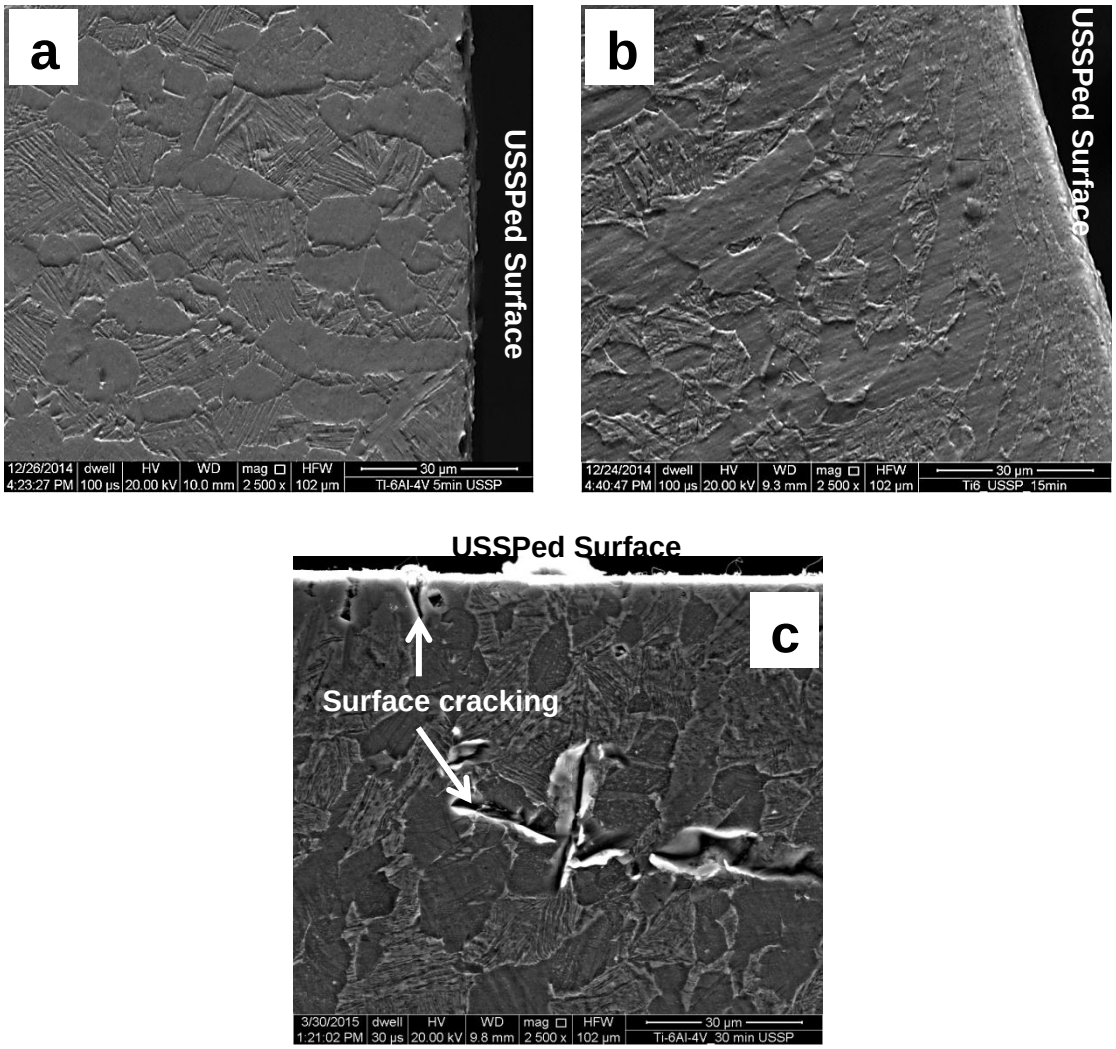

Fig. 3.4 SEM micrographs of the cross-sections of the specimens USSPed for (a) 5 minute, (b) 15 minute and (c) 30 minute.

3.2.3 Transmission Electron Microscopy

Transmission electron micrographs revealed the globular primary α and transformed β in the Ti–6Al–4V alloy in the ST condition (Fig. 3.5).

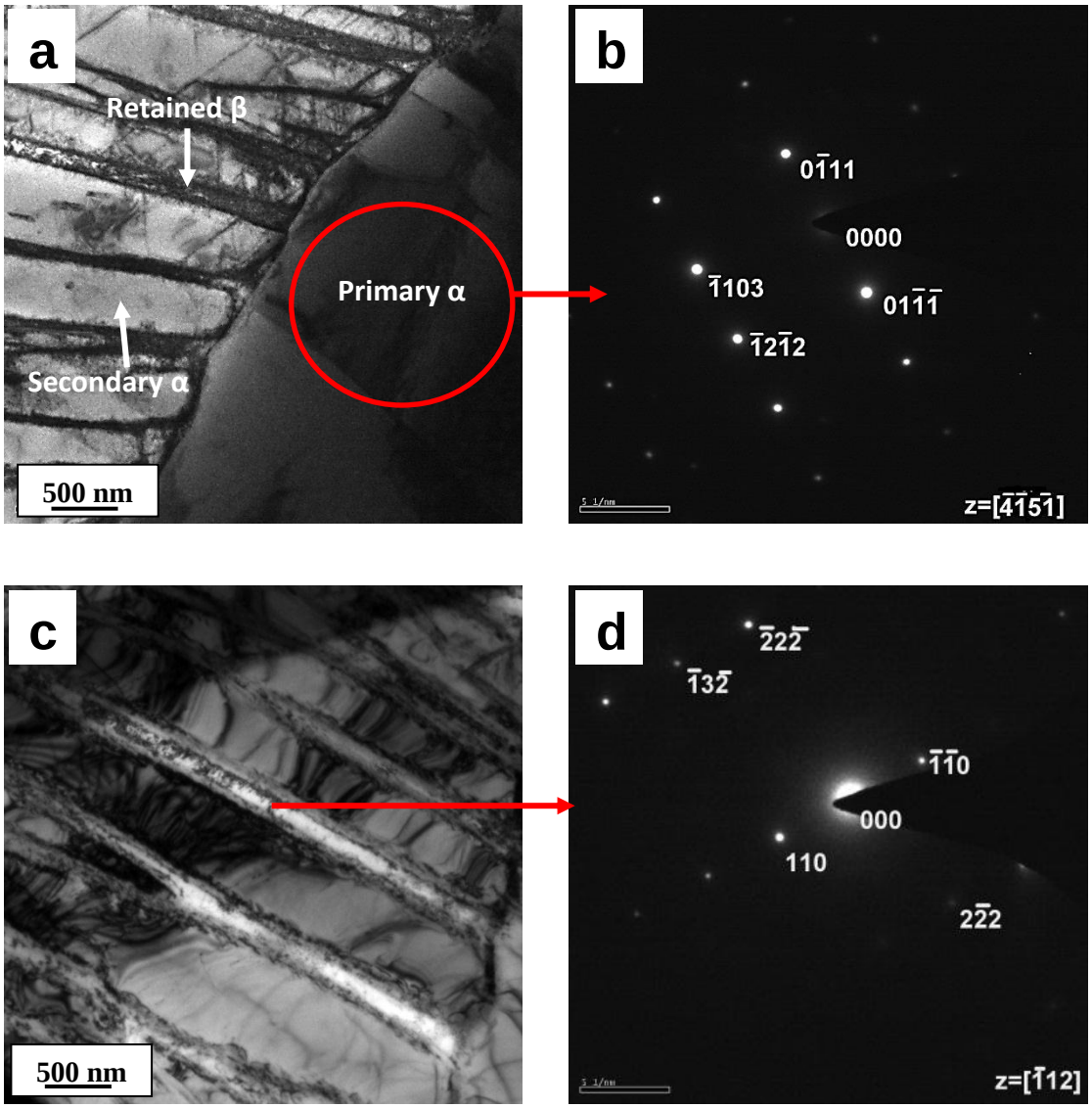

Fig. 3.5 Bright field TEM micrographs of the Ti–6Al–4V alloy in solution treated condition and the corresponding SAD patterns.

Figure 3.5a shows large primary α phase on the right side and transformed β phase on the left side containing long plate like features of secondary α phase along

with retained β phase, sandwiched between the α platelets. SAD pattern of the primary α phase is shown in Fig. 3.5b. Fig. 3.5c shows plate type features of secondary α phase and rod like features of retained β phase. The SAD pattern of the retained β phase is shown in Fig. 3.5d.

Figures 3.6, 3.7, 3.8 and 3.9 show TEM micrographs of surface regions of the samples subjected to USSP for 5, 10, 15, and 30 minute respectively. Fig. 3.10 shows TEM micrograph of surface region of the stress relieved (400 °C for 1h) 5 minute USSPed specimen. These bright field images are taken from the top surface regions of the shot peened samples. Grain refinement in the USSPed samples is quite obvious from the bright field images. The process of grain refinement in the surface layer involves severe plastic deformation from continual multidirectional mechanical impacts of steel balls at very high speed in surface region of the samples. Grain refinement is also obvious from the discontinuous ring pattern of the diffraction spots.

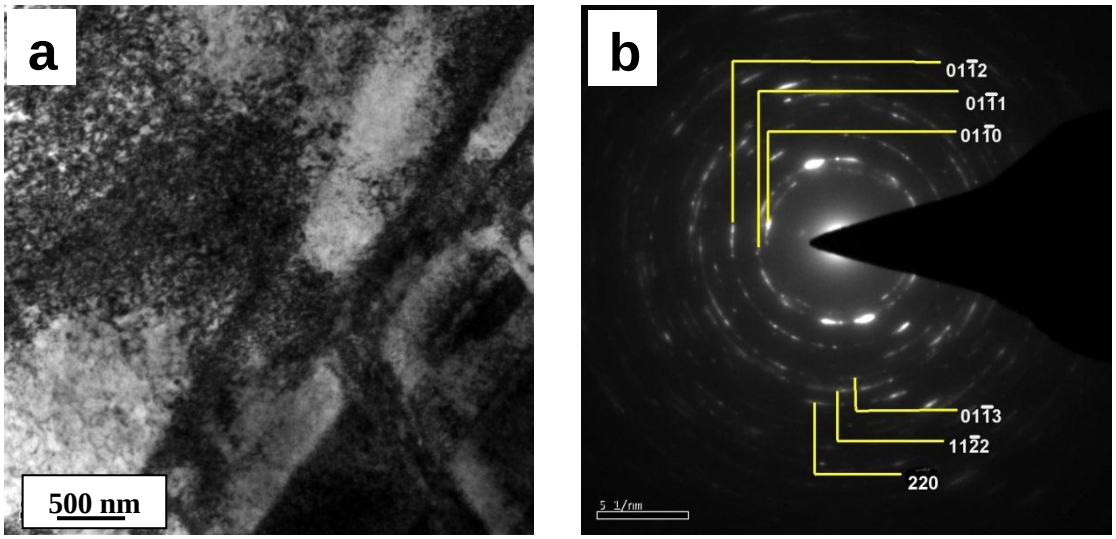

Fig. 3.6 Bright field TEM micrograph and the corresponding SAD pattern from surface region of the sample USSPed for 5 minute.

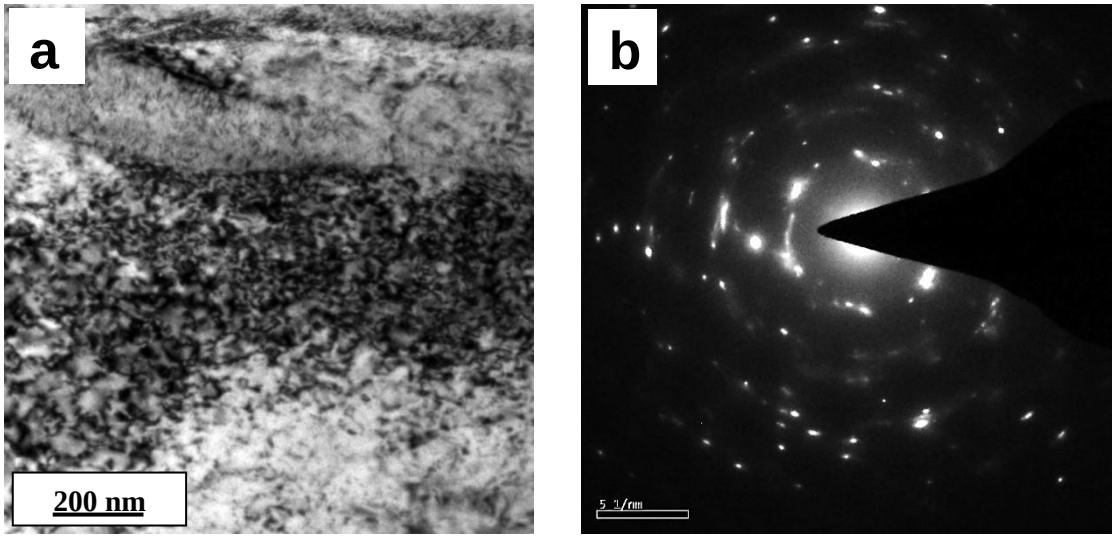

Fig. 3.7 Bright field TEM micrograph and the corresponding SAD pattern from surface region of the sample 5 minute USSPed+SR.

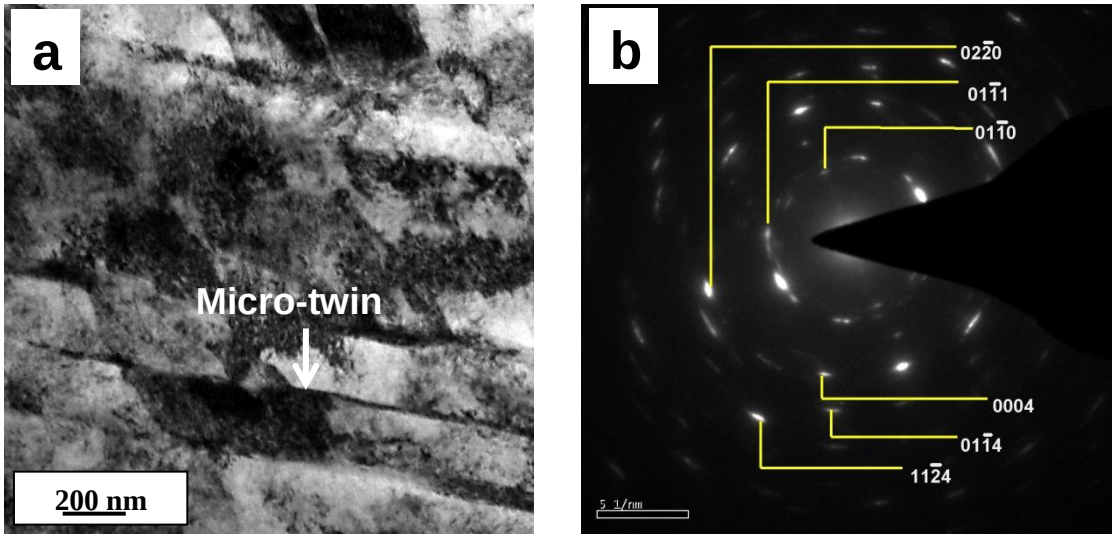

Fig. 3.8 Bright field TEM micrograph and the corresponding SAD pattern from surface region of the sample USSPed for 10 minute.

Micro-twins may be seen in parallel orientation in the sample shot peened for 10 minute, due to severe plastic deformation resulting from ultrasonic shot peening (Fig. 3.8a). Intersection of micro-twins was observed in surface regions of the 15 minute USSPed samples (Figs. 3.9a).

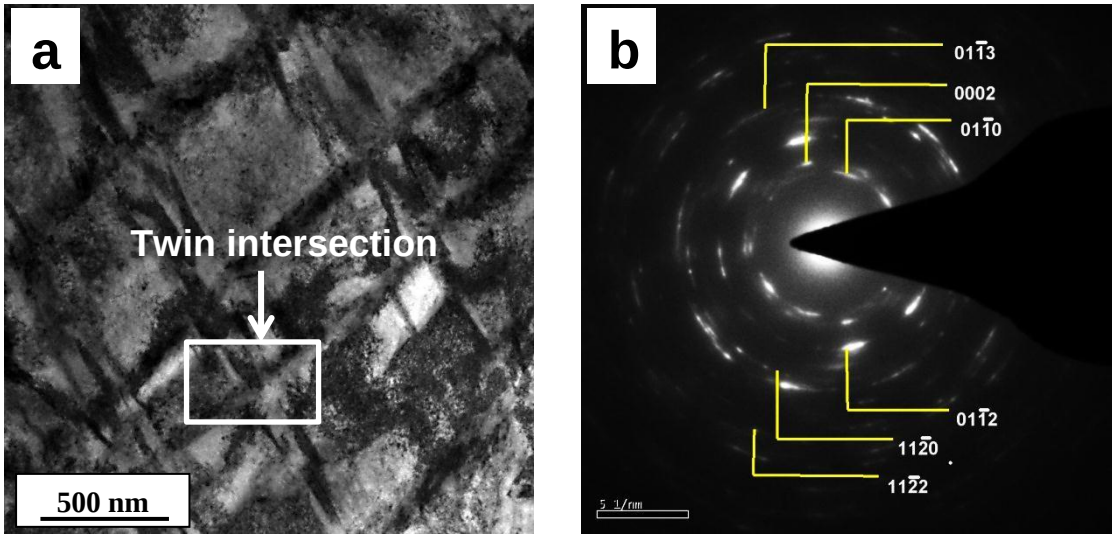

Fig. 3.9 Bright field TEM micrograph and the corresponding SAD pattern from surface region of the sample USSPed for 15 minute.

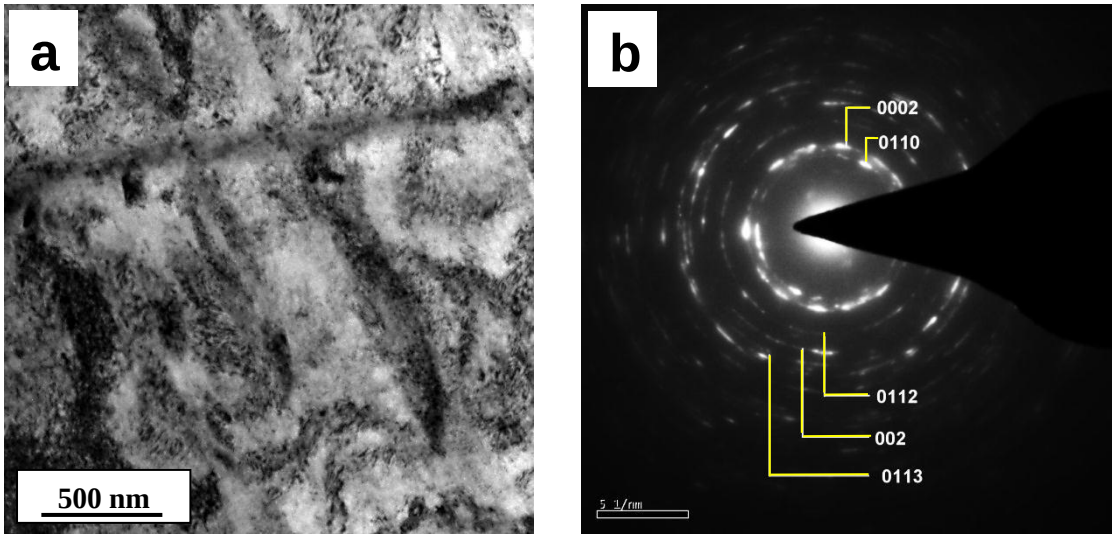

Fig. 3.10 Bright field TEM micrograph and the corresponding SAD pattern from surface region of the sample USSPed for 30 minute.

Intersection of micro-twins from severe plastic deformation resulting from USSP is quite obvious in the samples USSPed for 15 minute and adds to the process of refinement of the coarse grains into smaller grains of nano scale. It was found that size

of the grains was reduced with increasing duration of USSP. The calculated average grain sizes are recorded in Table 3.1.

Table 3.1 Average grain size in surface layer of the shot peened alloy Ti–6Al–4V measured from the TEM micrographs.

S. No.	USSP duration (minute)	Grain size (nm)
1.	5	21±4
2.	10	19±6
3.	15	17±3
4.	30	15±5
5.	5 minute USSPed+SR	21±8

3.3 XRD ANALYSIS

XRD analysis was carried out to study grain refinement, lattice strain, and characterization of phases. XRD profiles of the non-USSPed and the specimens USSPed for the different durations, showed only α and β peaks (Fig. 3.11), thus there was no phase change due to USSP. The Bragg diffraction peaks became broader for the USSPed specimens than that of the non-USSPed one. XRD profile also revealed that there was no phase change following the stress relieving (SR) treatment of the 5 minute USSPed sample (Fig. 3.12).

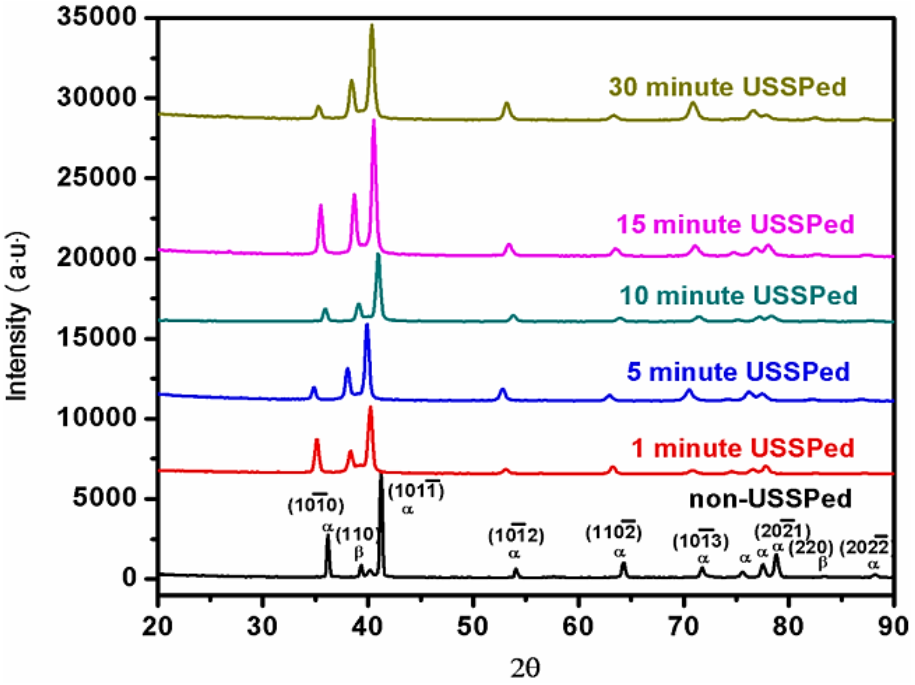

Fig. 3.11 X-ray diffraction of the alloy Ti–6Al–4V in the non-USSPed and USSPed for different durations.

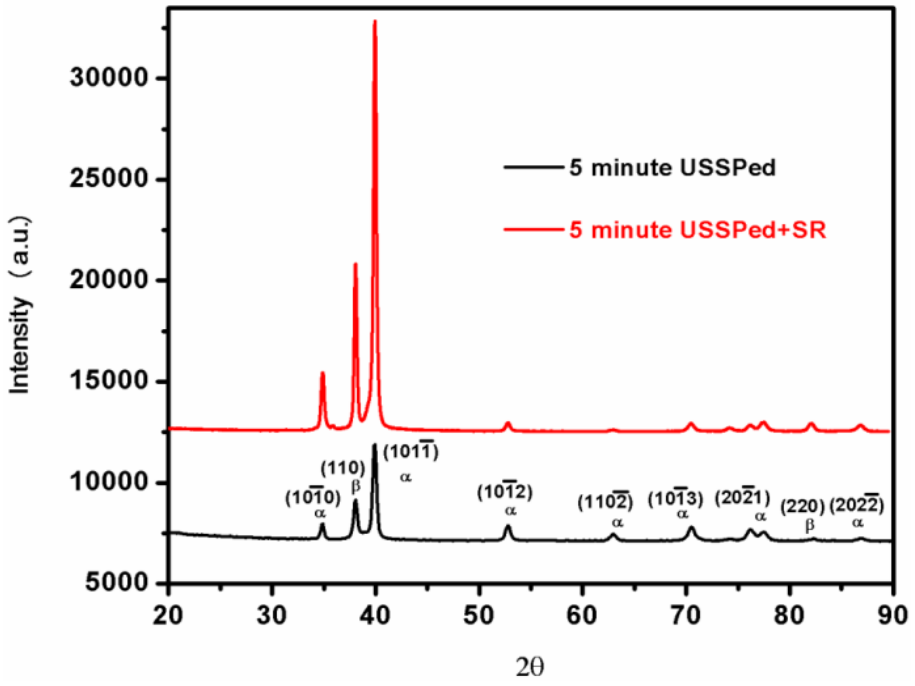

Fig. 3.12 X-ray diffraction of the material in USSPed and USSPed+SR conditions.

The average grain size and lattice strain of the USSPed samples were calculated from the diffraction line broadening of Bragg reflection peaks, using the Scherrer–Wilson and Williamson–Hall equations [Cullity (1956)].

$$\beta g\,(2\theta) = 0.9\lambda/D \cos(\theta) \quad \ldots\ldots\ldots\ldots\ldots\ldots \quad (3.1)$$

$$\beta g\,(2\theta) = 0.9\lambda/D + \varepsilon\, 4\tan(\theta) \quad \ldots\ldots\ldots\ldots\ldots\ldots \quad (3.2)$$

where θ is Bragg angle, D is average crystallite size, ε is lattice strain, λ is wavelength of the X-ray radiation and βg (2θ) is FWHM (peak width) following grain refinement in the sample.

The average grain size of the samples USSPed for 5, 10, 15, and 30 minute was found to be 25±3, 20±4, 18±4 and 16±3 nm, respectively. The average grain size was observed to decrease and Bragg peaks to broaden with increase in the duration of USSP. However, little change was observed in grain size following the SR treatment. The calculated average grain size and the lattice strain after USSP are listed in Table 3.2. Similar trend was observed also in the lattice strain. The diffraction peaks also revealed features characterizing internal strain developed due to micro distortion of the lattice. It was observed that internal strain varied with the duration of USSP. The calculated lattice strain was much smaller than that of the nano crystallized by other process like severe plastic deformation [Horita et al. (1998)].

Table 3.2 Average grain size and lattice strain in surface layer of the shot peened alloy Ti–6Al–4V.

S. No.	USSP duration (minute)	Grain size (nm)	Lattice strain (%)
1.	1	35±5	0.357
2.	5	25±3	0.496
3.	10	20±4	0.500
4.	15	18±4	0.501
5.	30	16±3	0.588
6.	5 minute USSPed+SR	26±5	0.489

3.4 SURFACE ROUGHNESS

The typical surface profiles of the USSPed and non-USSPed samples are shown in Fig. 3.13 and the surface roughness parameters are recorded in Table 3.3. The average surface roughness (Ra) was determined using profilometer and was found to increase with increase in the duration of USSP. Highest surface roughness was observed for the 30 minute USSPed sample. However, all the USSPed samples showed higher surface roughness in comparison with that of the non-USSPed one.

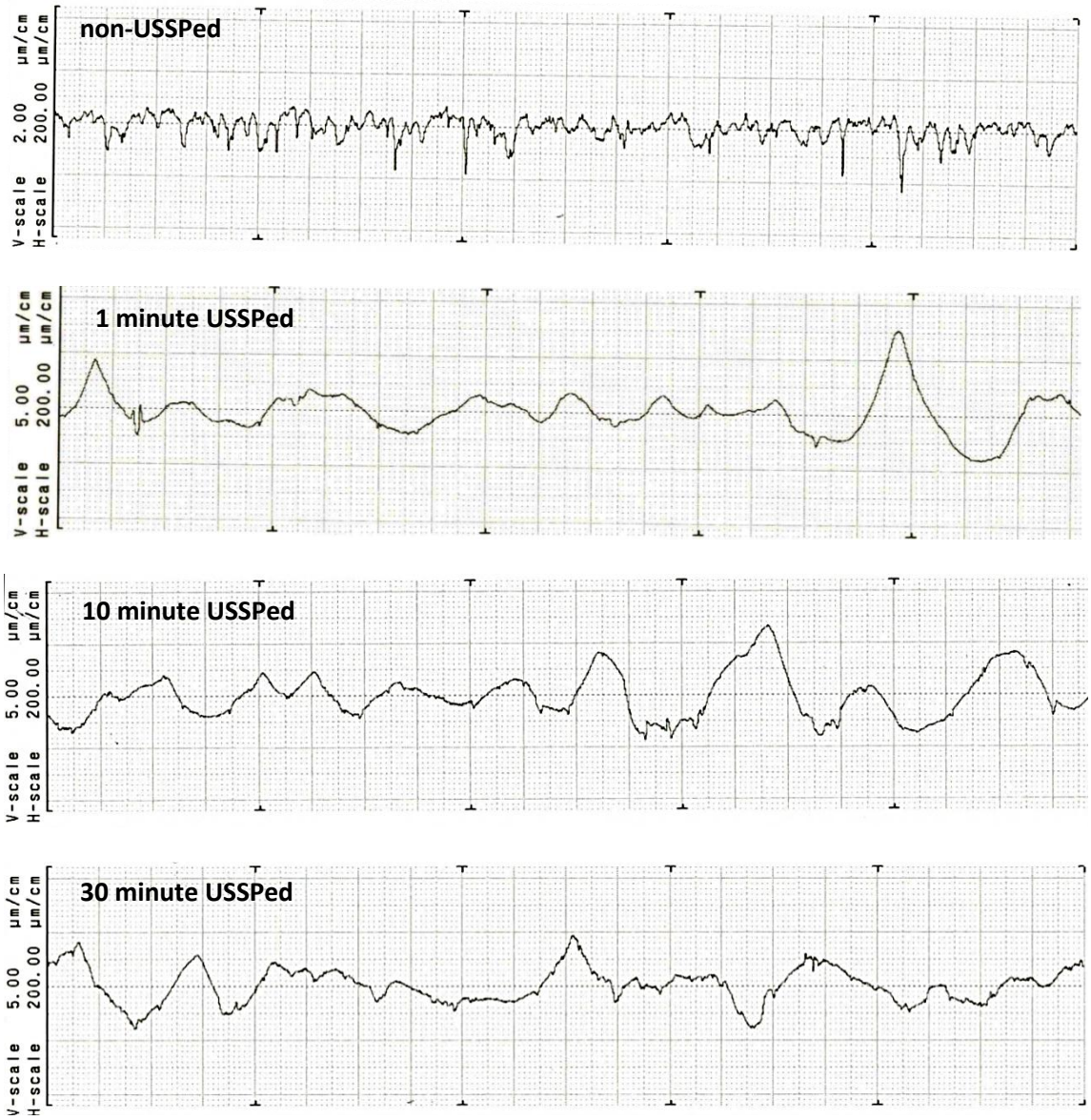

Fig. 3.13 Surface roughness profiles with different durations of USSP.

Table 3.3 Surface roughness of the non-USSPed and USSPed samples for different durations of USSP of the alloy Ti–6Al–4V.

S. No.	USSP duration (minute)	Surface roughness (μm)		
		Ra	Rq	Rz
1.	0	0.196±0.006	0.284±0.009	2.172±0.216
2.	0.25	1.011±0.017	1.349±0.013	4.995±0.279
3.	0.5	1.040±0.019	1.361±0.016	5.467±0.268
4.	1	1.049±0.008	1.390±0.011	5.471±0.251
5.	2.5	1.069±0.015	1.427±0.017	5.599±0.241
6.	5	1.105±0.018	1.452±0.021	5.821±0.289
7.	7.5	1.210±0.014	1.531±0.018	5.877±0.301
8.	10	1.231±0.019	1.548±0.026	5.927±0.225
9.	15	1.295±0.027	1.574±0.029	6.943±0.266
10.	30	1.714±0.039	1.886±0.036	7.409±0.273

Ra= Roughness average

Rq=Root mean square (RMS) roughness

Rz= Average maximum height of the profile

3.5 MICROHARDNESS PROFILE

Figure 3.14 shows variation of microhardness of the specimens from the shot peened surface towards interior. The shot peened samples were sectioned in two halves along their diameter, perpendicular to the shot peened surface. The average microhardness of the non-USSPed specimen was found to be 504 HV.

Microhardness was found to increase progressively with the duration of shot peening and hardness values of those specimens USSPed for 5, 15 and 30 minute were 531, 618 and 678 HV respectively, at the USSPed surfaces. Microhardness of the samples USSPed for 30 minute was increased by ≈34%. The microhardness was found to vary significantly up to the depth of ~100 µm. After the stress relieving treatment, surface microhardness of the 30 minute USSPed sample was reduced by 14% to 603 HV, however, it was still higher by ~20% than that of the non-USSPed surface. The microhardness data did not consider the indentation effect, if any.

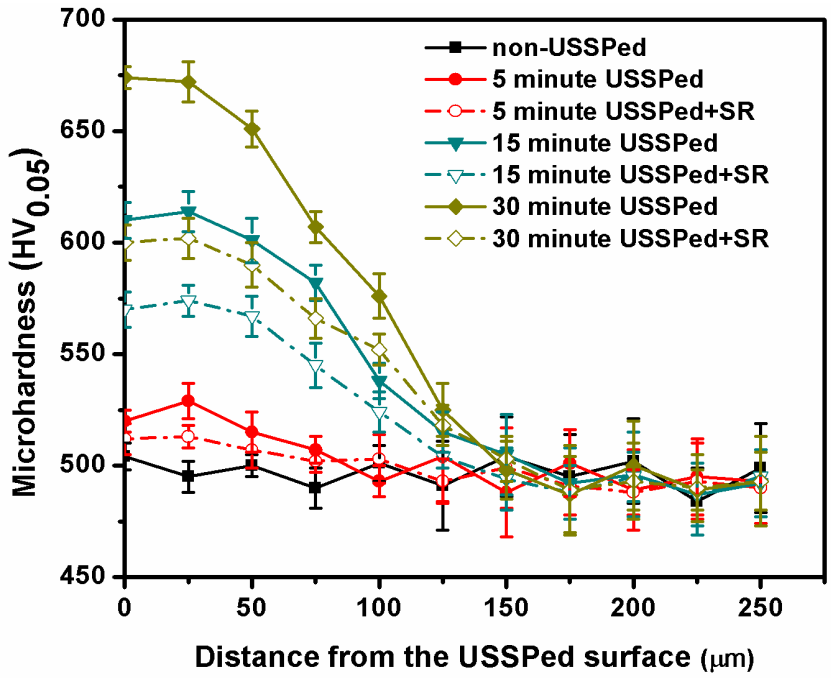

Fig. 3.14 Variation of microhardness of the non-USSPed, USSPed and USSPed+stress relieved specimens from surface towards interior.

3.6 RESIDUAL STRESS

The compressive residual stress in surface region of the USSPed sample showed progressive increase with depth from the USSPed surface and attained the maximum

value of 620 MPa at the depth of ≈200 μm; however, it decreased at the higher depth (Fig. 3.15). The residual stress became tensile in nature beyond this depth and increased with depth to reach 10 MPa at the depth of 400 μm following the SR treatment.

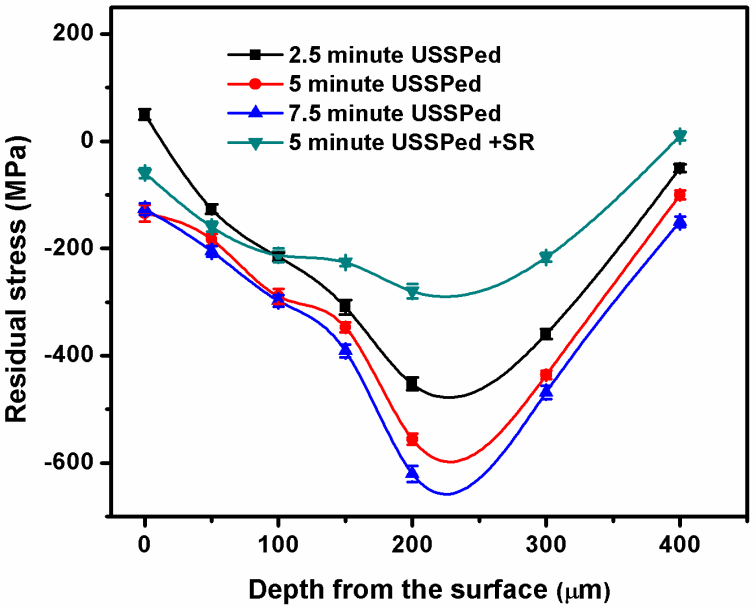

Fig. 3.15 Variation of residual stress from the treated surface towards interior of the USSPed and USSPed+SR sample.

3.7 DISCUSSION

A typical two phase microstructure consisting of globular α and transformed β in the α+β solution treated condition is quite obvious from the optical and SEM micrograph (Fig. 3.1). The impingement of hardened steel balls on flat surface of the alloy Ti–6Al–4V induced severe plastic deformation in the surface region at high strain rate. The thickness of the surface layer, deformed by USSP increased with peening duration and was found to be ~200 μm for the 30 minute USSPed specimen (Fig. 3.2d). Shot peening for long duration of 30 minute was found to cause surface cracking (Fig.

3.4c) due to excessive work hardening in very thin region of the surface, induced by Hertzian contact strain generated by spherical balls on the planar surface.

The tendency of surface cracking due to USSP depends on the nature of material, for example, materials with low stacking fault energy like high nitrogen austenitic stainless steel was observed to crack from USSP even for the duration of less than 10 minute [Rai et al. (2014)]. Materials with low stacking fault energy work harden rapidly and undergo cracking due to excessive work hardening, in particular at high strain rates.

The features of primary α and transformed β are more distinct from the TEM micrograph (Fig. 3.5a). The transformed β phase, consisting of platelets of secondary α and thin strip of retained β, sandwiched between the α platelets, may clearly be seen from the TEM micrograph (Fig. 3.5c). The aligned morphology of secondary α platelets in transformed β in the non-USSPed condition was highly distorted and modified due to USSP treatment (Figs. 3.6, 3.8, 3.9 and 3.10). There was no significant change in grain size following the stress relieving treatment (Fig. 3.7).

USSP of the material for 5, 10, 15 and 30 minute may be seen to produce nano size grains in the surface region. The SAD pattern of USSPed samples showed partially developed circles with well-defined diffraction spots, indicating grain refinement (Fig. 3.6b, 3.7b, 3.8b, 3.9b and 3.10b). The refinement of initial grains of ~12 μm size into nano scale from USSP may be understood in terms of severe plastic deformation, twinning, intersection of twin systems, and further breakdown of submicron grains into nano grains [Zhu et al. (2004)]. Twinning is a planar defect in nanocrystalline structure resulting from the severe plastic deformation at very high strain rate.

Twinning occurs when there are insufficient slip systems to accommodate the deformation and the material has low stacking fault energy. The role of micro-twinning in grain refinement of low stacking fault energy materials has earlier been discussed at length [Tao et al. (2004), Lu. et al. (2004)]. Since the alloy Ti–6Al–4V is a material of low stacking fault energy [Miao et al. (2013)], the mode of plastic deformation changed from dislocation slip to mechanical twinning. Twins are of primary importance in conversion of coarse grained structure into nanostructure as they progressively subdivide the original grains into smaller grains [Wang et al. (2006), Lu et al. (2009)].

Progressive division of the original coarse grains by twin boundaries and sub-boundaries leads to formation of nano grains. These twins resulting from USSP formed because of severe plastic deformation. Development of micro-twins as well as their intersection in the specimens USSPed for 10 and 15 minute is shown in Figs. 3.8a and 3.9a, respectively. Formation of micro-twins resulted from continual multidirectional mechanical impacts of steel balls on surface of the material at very high speed and increase in the lattice strain. Lattice strain was higher in the sample shot peened for 30 minute than in those shot peened for 5, 10 and 15 minute. The typical grain sizes of about 21±4, 19±3, 17±3 and 15±5 nm resulted in the samples shot peened for 5, 10, 15, and 30 minute respectively. Clustering of SAD spots in some rings indicates that many nano grained regions had common crystallographic orientation, suggesting that these nano grains developed from the large size grains.

It was confirmed from the X-ray diffraction analysis that there was no phase change even after 30 minute of USSP and SR treatment (Figs. 3.11 and 3.12). Bragg diffraction peak broadening from USSP, established formation of nanostructure in the surface region. The broadening of diffraction peaks due to USSP treatment suggests

grain refinement and/or an increase in the atomic level lattice strain [Miao et al. (2013), Pandey et al. (2015)]. It may be seen that as the duration of shot peening increased Bragg peaks broadened and the grain size was reduced. The grain size determined by TEM was smaller than that determined from X-ray diffraction (Tables 3.1 and 3.2). It may be due to the fact that depth of the nanostructured surface layer was smaller than the depth detectable by X-ray diffraction. Rai et al. (2014) also observed grain refinement in high nitrogen austenitic stainless steel and found decrease in crystallite size with increase in the processing time from 1.5 to 13.5 minute.

The surface roughness was found to be higher on the sample USSPed for 30 minute (Table 3.3). The USSPed specimens showed significant increase in microhardness. It was found to be increased up to the depth of ≈100 μm with increase in peening duration (Fig 3.14). The 34% increase in microhardness on the surface of the sample USSPed for 30 minute was due to associated compressive residual stresses and grain refinement to nano level. Shadangi et al. (2015) proposed that microhardness was increased due to grain refinement, increase in dislocation density and decrease in twin spacing. The hardness of USSPed sample was higher than that of the non-USSPed one even after the stress relieving treatment which implies that change in hardness was not only due to the compressive residual stresses but also due to grain refinement. The compressive residual stresses increased with increase in peening duration. It was highest (620 MPa) at the depth of 200 μm.

3.8 CONCLUSIONS

Surface nanostructuring of the alloy Ti–6Al–4V was induced through USSP technique. The grain refinement occurs from the combined process of mico-twinning

and intersection of twins. Also the microhardness was increased due to USSP and compressive residual stress was induced in surface region of the material.

Following conclusions are drawn from this chapter:

1) Nanograins in the range of 15-21 nm developed in the alloy Ti–6Al–4V by USSP with hard steel balls of 3mm diameter.
2) Surface roughness was increased with increase in the duration of USSP.
3) Micro-twins and intersection of twins resulted due to USSP.
4) There was no effect of USSP on phase stability of the alloy as no additional phase was detected through XRD following USSP.
5) There was appreciable increase in microhardness of the USSP affected region.
6) Microhardness profile of the USSPed region was raised with increase in the duration of USSP treatment.
7) A compressive residual stress of 620 MPa was produced at the depth of ≈200μm from USSP.